IOP Conf. Series: Materials Science and Engineering **724** (2020) 012008 doi:10.1088/1757-899X/724/1/012008

Proposed parameter for the characterization of friction in cylindrical gears teeth contact

S Alaci[1], C Bujoreanu[2], N D Petrea[2], F C Ciornei[1], L Irimescu[1]

[1]Department of Mechanics and Technologies, „Stefan cel Mare" University, Suceava, Romania

[2]Department of Mechanical Engineering, Mecahatronics and Robotics, „Gheorghe Asachi" Technical University, Iasi, Romania

Abstract. Gear mechanisms are widely used in technical applications, mainly for transmitting rotational motion between two axes with constant transmission ratio via a higher pair. Significant friction energy loss in the pair between teeth highlights the importance of estimating the mechanical work lost by friction within this contact. In a previous study, the coefficient of rolling friction between a cylindrical body and a flat face body was found based on the decrease of oscillations amplitude of a cycloidal pendulum. The basic idea of the present paper follows the observation that in the case of a gear mechanism, the relative motion between the wheels can be taken as relative motion of their axodes. In this regard, a pendulum obtained from a mobile cylindrical gear with attached rod and a fixed corresponding rack is considered. The law of motion of the cycloidal pendulum is applied for the proposed pendulum and an "equivalent rolling friction coefficient" which characterises the friction between the teeth of the pinion and the rack is found. The differential equation modelling the motion of the pinion-rack pendulum is difficult to obtain, which is explained by the analysis of the involute gear field of a general cylindrical gear mechanism.

1. Theoretical considerations

The gearing phenomenon occurring between two geared wheels is quite complex [1-2] Several aspects should be considered for the proper running of a gear mechanism, such as continuity of action, avoiding primary interference, secondary interference, radial clearance limitation etc. In figure 1, the gearing field of an involute gearing [3] is presented. The gearing process takes place in the region between the addendum circles of the wheels, c_{a1} and c_{a2}.

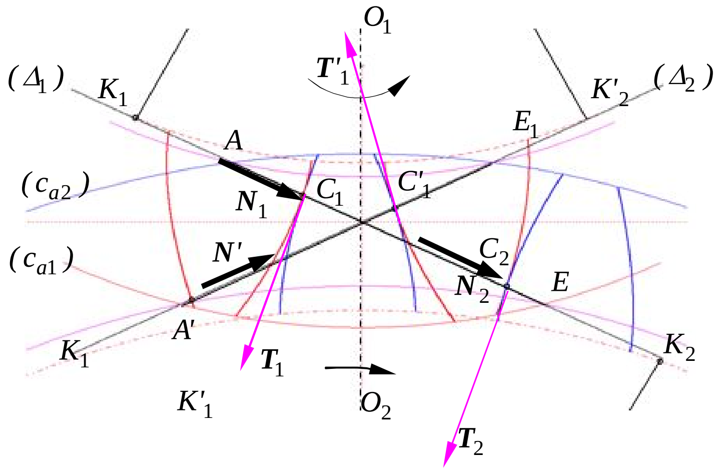

Figure 1. The gearing field of an involute gearing.

The contact points between wheels move along the lines of action K_1K_2 and $K'_1K'_2$, which are common tangents to the base circles. In the case when the pinion is denoted 1, the points where the force between the wheels is transmitted are C_1 and C_2, the gearing starts in point A and ends in point E. The normal lines in the contact points are directed along the straight line K_1K_2 while the friction forces $\boldsymbol{T}_1$ and $\boldsymbol{T}_2$ are perpendicular to the line of action. In the instance when wheel 2 becomes the driving one, with the rotation direction as in figure 1 the point where the force is transmitted is C'_1 from $K'_1K'_2$, the gearing starts in the point A' and ends in the point E', the normal force $\boldsymbol{N}'_1$ is now along the straight line K'_1K_2 and the friction force $\boldsymbol{T}'_1$ is normal to it. Regardless of which wheel is the driving one, the gearing is double point contact at the ends of the segment of action, while in the vicinity of the gearing pole, it is single point contact. During the double point contact gearing, the mechanical system becomes statically undetermined, since from the equations of equilibrium only the sum between the magnitudes of the normal forces can be found. This results in the difficulty in estimation of the friction forces between the flanks.

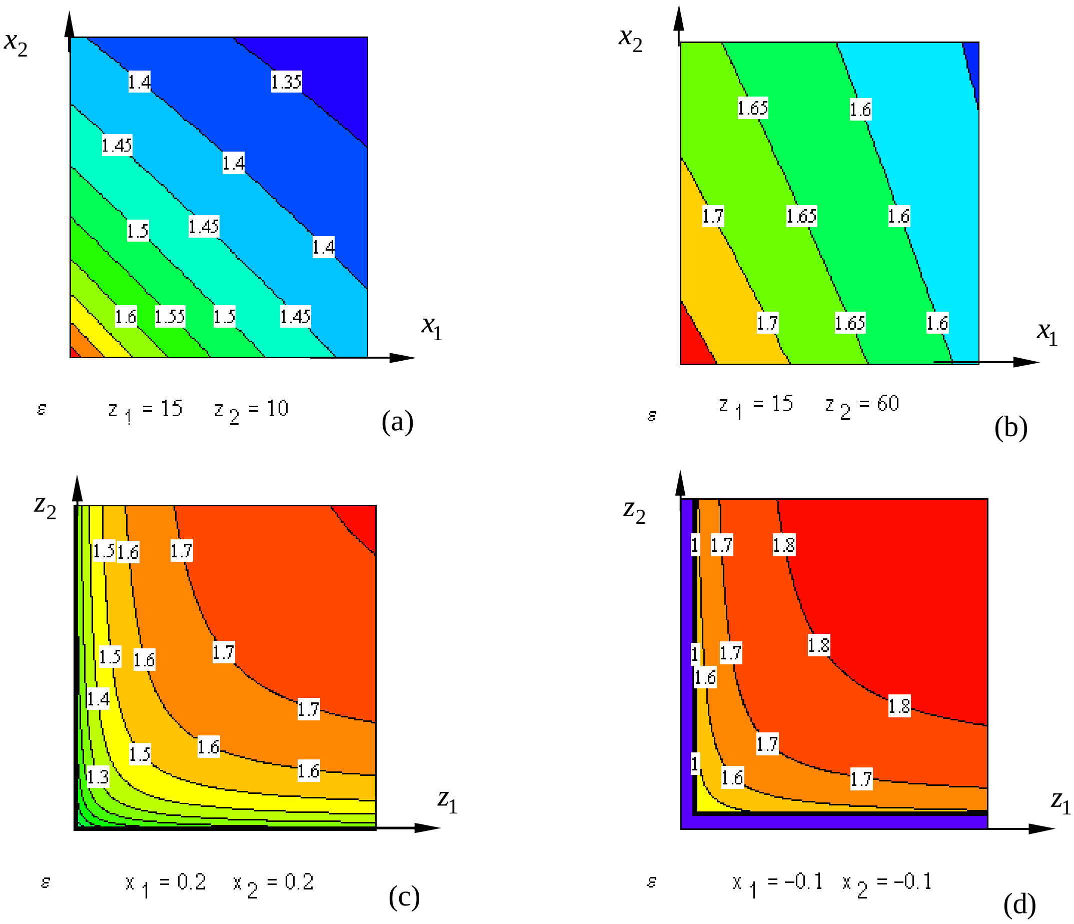

Figure 2. The effect of profile shifts (a), (b) and of number of teeth (c), (d) upon the contact ratio.

The ratio between the periods of uni-point and double-point contact gearing is characterised by ε, the contact ratio [4]. The higher the contact ratio, the greater the percentage of double point contact gearing. In figure 2, the effects of the variance of number of teeth and of the profile shifts upon the contact ratio ε are presented. Regardless of the two wheels' parameters values, the double point contact gearing is always present; therefore, the friction between the flanks of the teeth is always difficult to characterise.

2. Principle of the method. Theoretical model

In engineering applications, an estimation of the global effect of friction forces is seldom required, instead the instantaneous values of the friction torsor is preferred. For this purpose, we start from the

IOP Conf. Series: Materials Science and Engineering **724** (2020) 012008 doi:10.1088/1757-899X/724/1/012008

remark that during the gearing process, the relative motion of the wheels is completely characterized by the motion between the axodes of the relative motion. In [5], based on the hypothesis of proportionality between the normal force and the rolling friction torque, the coefficient of rolling friction was found using a cycloidal pendulum made by a spherical end rolling on a plane surface.

For the purpose of this paper, for the pinion-rack gearing, the axodes of the motion are the pitch cylinder and the rolling plane of the rack. The cycloidal pendulum from figure 3 is used in characterizing the friction between the flanks of the pinion and the rack. A circle of r radius, the pitch radius of the wheel, rolls with no slip over a straight line Δ_0. G is the centre of mass of the pendulum, M is the mass of the pendulum and d is the distance with respect to the centre of the circle. The central moment of inertia of the pendulum is J_G. The normal reaction $\boldsymbol{N}$, the friction force $\boldsymbol{T}$ and the rolling friction torque M_r act at the contact point between the circle and the straight line:

$$M_r = s_r N \tag{1}$$

where s_r is the coefficient of rolling friction. Under the assumption of pure rolling in the contact point, the position of the pendulum is given by the angle φ between the straight line through the centre of the circle and the centre of mass and the vertical direction:

$$\ddot{\varphi} = -\frac{(r\sin\varphi / d + s_r \cdot \cos\varphi \, sgn\dot{\varphi} / d)\dot{\varphi}^2 + (s_r \, sgn\dot{\varphi} / d + \sin\varphi) g / d}{1 + J_g / Md^2 + s_r \cdot \sin\varphi \, sgn\dot{\varphi} / d - 2r\cos\varphi / d + r^2 / d^2} . \tag{2}$$

The equation (2) is nonlinear and must be integrated numerically. It is necessary to stipulate the initial amplitude of the pendulum, φ_0 and the angular velocity ω_0. For $s_r = 0$ and $r \to 0$ the above equation is simplified as:

$$\ddot{\varphi} = -\frac{g\sin\varphi / d}{1 + J_G / Md^2} = -\frac{Mgd\sin\varphi}{J_G + Md^2} = -\frac{Mgd\sin\varphi}{J_O} . \tag{3}$$

Equation (3) is the equation of motion of the physical pendulum, oscillating about an axis passing through O which validates equation (2). After integration, the magnitude of the normal force N and of the friction force T from the contact point C are found applying the relations:

$$N = \ddot{\varphi} Md\sin\varphi + \dot{\varphi}^2 Md\cos\varphi + Mg \tag{4}$$

$$T = \ddot{\varphi} M(r - d\cos\varphi) + \dot{\varphi}^2 Md\sin\varphi \tag{5}$$

3. Experimental set-up. Description and functioning

In figures 3 and 4, the experimental device is shown; it consists of a rack 1 of module $m = 2$ (mm), fixed horizontally on the working table by two rods of square cross-section. A mobile pinion with $z = 50$ is gearing the fixed rack. During the pinion-rack gearing, the pitch circle of the pinion rolls without sliding over the pitch line of the rack, therefore the points of the wheel describe a family of cycloids.

Two aluminum rods 2 in which equidistant holes were made (the arm) are fixed on the pinion 3 and on the cylindrical part (the bob) from the lower end of the pendulum. When the pinion and the rack teeth are brought into contact as a gear mechanism (the pivot), a cycloidal pendulum which oscillates under its own weight is obtained. As shown above, the position of the pendulum is entirely given by the angle made by the straight line passing through the centers of the pinion and of the bob with the vertical direction. In order to find the tilt angle of the pendulum, a small laser pointer 4 is attached, tangent to the pitch circle of the pinion and normal to the arm. The displacement of the spot emitted by the laser pointer can be estimated on a vertical ruler 5, fixed at a distance D from the axis of the vertical pendulum.

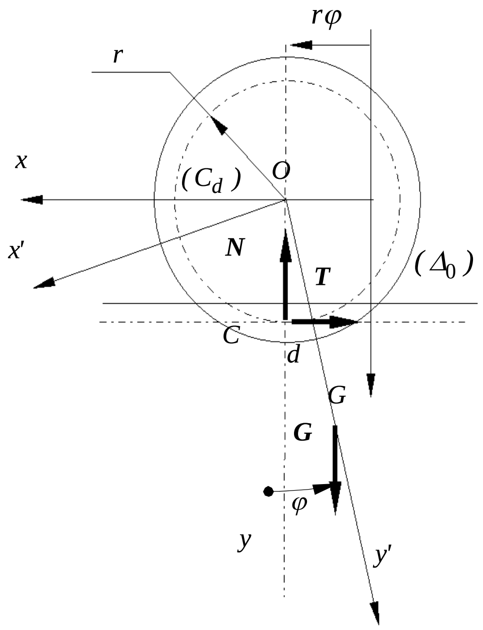

Figure 3. The principle scheme of the device.

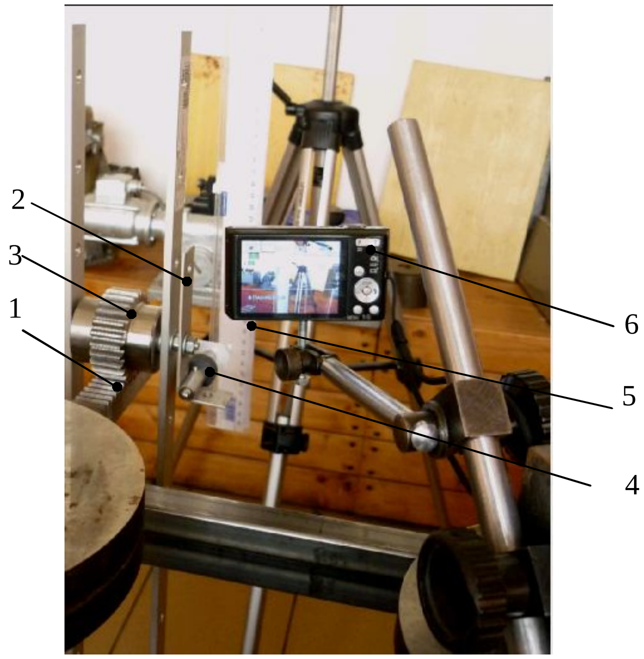

Figure 4. The actual device.

The motion of the mobile spot along the ruler is filmed using a camera 6. The moments when the spot attains the extreme positions can be precisely identified by analyzing the frames of the film. Thus is obtained the law of variation of the amplitude of the spot oscillation.

$$z_k = z_k(t_k) \tag{6}$$

By neglecting the effect of the horizontal displacement of the pinion during the oscillation, the angular amplitude of the pendulum can be expressed as:

$$\theta_k = atan\frac{z_k - z0}{D} \tag{7}$$

where $z0$ is the coordinate of the laser spot for the immobile pendulum. The angular amplitude of the pendulum versus time described by relation (7), obtained experimentally, is presented in figure 5. *The linear decrease of the amplitude validates that the attenuation of the motion is due only to the dry friction* as shown in [6-7]. When other responsible factors occur, the shape of the plot is curved.

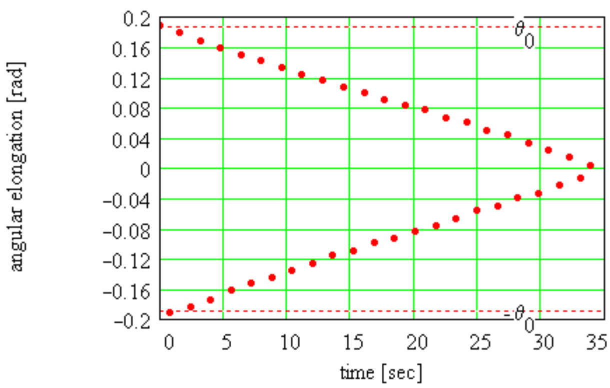

Figure 5. The experimental variation of the angular amplitude of the pendulum.

4. Finding the characteristic parameter of the friction between the flanks

The parameter that characterizes the friction of the pivot of the pendulum, named "equivalent rolling friction coefficient" since provides a global illustration of the friction phenomenon in the teeth contact and denoted by s, is obtained following the methodology presented in [5]. In brief, the equation of motion of the pendulum is numerically integrated with the following imposed initial conditions:

$$\varphi\big|_{t=0} = \theta_0; \;\; \omega\big|_{t=0} = 0 \tag{8}$$

where θ_0 is the maximum value of experimental amplitude. Subsequently, the value of equivalent rolling friction coefficient s is found by trials from the condition that the theoretical solution passes through the experimental points. In order to integrate the equation of motion (2), the mass of the pendulum M, the position of the center of mass with respect to the center of the pinion d and the moment of inertia J_G with respect to an axis parallel to the axis of oscillation passing through the center of gravity G are required. The mass M is found through weighting and the value obtained is $M = 2.837kg$. The position of the center of mass and the moment of inertia J_G were obtained (as in [5], [8]) and $d = 0.480m$ was obtained. The central moment of inertia was found based on the period of oscillation of the physical pendulum. From the oscillations of the pendulum about the shaft results the period of oscillation T_0:

$$T_0 = \frac{nr.frames \cdot times\_of\_frame}{nr.ocilations} = \frac{1563\,frames \cdot (1/30)\,sec}{30\,oscillations} = 1.737\,sec \tag{9}$$

The physical pendulum's expression of period leads to the value of the central moment of inertia J_G:

$$J_G = \left(\frac{g\zeta\, T_0^2}{4\pi^2} - \zeta^2 \right) M = 0.302\,kg \cdot m^2 \tag{10}$$

The equation of motion (2) was integrated using the above data, for several values of the friction parameter (equivalent rolling friction coefficient) s; after some trials (following the methodology from [9-10]) the value $s = 0.00105$ proved an excellent interpolation of the experimental data, as shown in figure 6. Full concordance is observed between the period of oscillation of the experimental pendulum and the period of the theoretical model. Another remark that should be highlighted concerns the sensibility of the interpolation curves versus the parameter of friction s. In order to support the affirmation, the plots from figure 7 are presented, where the value of the s parameter was modified by 5% in both directions. As expected, the normal force differs slightly from the weight Mg of the pendulum and it can be considered constant.

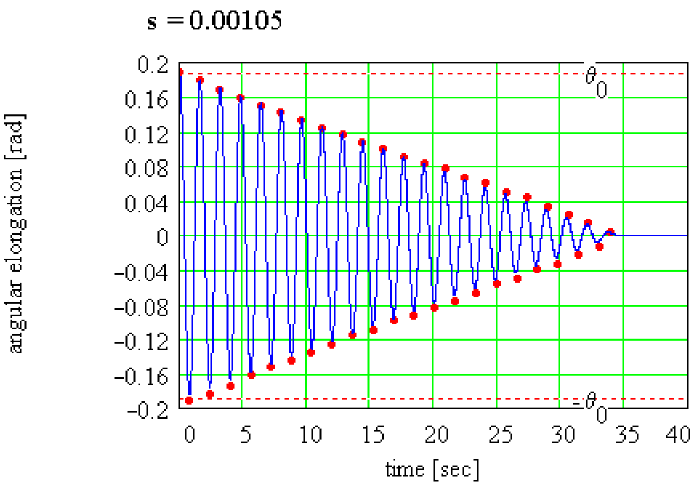

Figure 6. The interpolation of experimental data with the solution of the equation of motion, and establishing the parameter of friction.

Concerning the friction force, its amplitude decreases linearly, and in the points of maximum elongation, finite discontinuities exist, characteristic to the transition from dynamic to static friction.

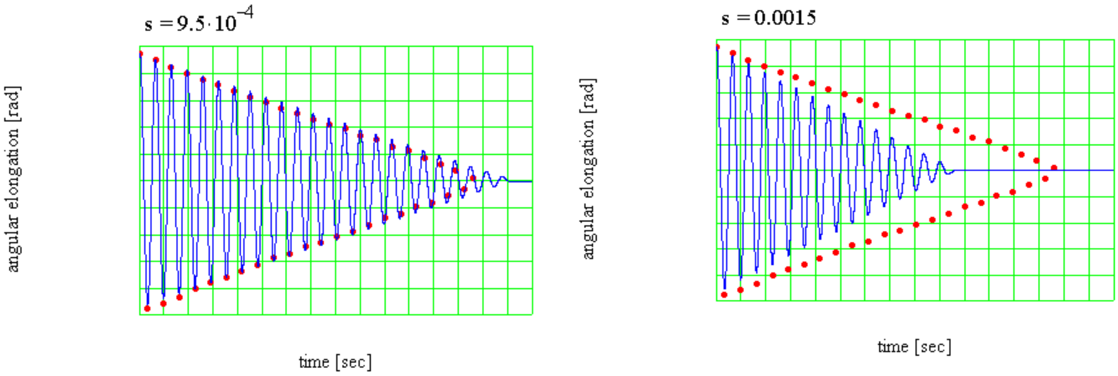

Figure 7. The effect of the coefficient s upon the solution of the theoretical model.

5. Conclusions

The paper presents a method for the estimation of the friction between the flanks of cylindrical gears with the concrete example of application on spur gears. An experimental device was designed and constructed, based on the method of finding the coefficient of rolling friction between a sphere and a plane, and on the remark that the motion between a pinion and a rack can be replaced by the motion of rolling without sliding between the pitch circle and the rack's line of action. The device consists of a pendulum for which the pinion- rack contact is the pivot. For this pendulum, the linear decrease of angular amplitude is obtained experimentally, attenuation for which only the dry friction between the flanks of the gear is responsible. The experimental data are interpolated with the signal generated by the integration of the cycloidal pendulum's equation of motion, and the "coefficient of rolling friction" correlated to the actual pendulum is found. This global parameter allows for the quantitative comparison of frictions occurring in different pairs of gears. This parameter can be employed for the global characterization of friction between the pinion-rack flanks. The effects of the gear parameters - like the module, the rack shift coefficient, and the inertial characteristics of the pendulum upon the "equivalent rolling friction coefficient" are intended for future work.

6. References

[1] Rider M J 2015 *Design and Analysis of Mechanisms: A Planar Approach* 1st Ed Wiley 316 p
[2] Sclater N 2011 *Mechanisms and Mechanical Devices Sourcebook* 5th Ed McGraw-Hill Education p560
[3] Handra Luca V and Stoica I A 1982 *Introduction in the theory of mechanism* (in Romanian *Introducere in teoria mecanismelor*) Vol. I Ed Dacia Cluj
[4] Maros D 1958 *Kinematics of gear mechanisms* (in Romanian *Cinematica Rotilor Dintate)* Ed Tehnica Bucuresti p327
[5] Ciornei M-C, Alaci S, Ciornei F-C and Romanu I-C 2017 *IOP-MSE* **227** 012027
[6] Torzo G and Pearnzoni P 2009 The real pendulum: theory, simulation, experiment *Lat. Am. J. Phys. Educ*. **3**(2) pp 221-228
[7] Zonetti L F C, Camargo S S, Sartori J, de Sousa D F and Nunes L A O 1999 A demonstration of dry and viscous damping of an oscillating pendulum *Eur. J. Phys*. **20** pp 85–88
[8] Hibbeler R C 2015 *Engineering Mechanics: Dynamics* 14th Ed Pearson p784
[9] Alaci S, Ciornei F-C, Bujoreanu C,Ciornei M-C and Acsinte I-L 2018 doi: 10.1088/1757-899X/444/2/022015 *IOP-MSE* **444** 022015
[10] Alaci S, Ciornei F-C, Ciogole A and Ciornei M-C 2017 doi:10.1088/1757-899X/200/1/012005 *IOP-MSE* **200** 012005

Acknowledgement
This work was supported by a grant of the Romanian Ministry of Research and Innovation, CCCDI – UEFISCDI, project number PN-III-P1-1.2-PCCDI-2017-0404 / 31PCCDI/2018, within PNCDI III.